Surface state conductivity in epitaxially grown $Bi_{1-x}Sb_x$ (111) films

2016 New J. Phys. 18 093012

(http://iopscience.iop.org/1367-2630/18/9/093012)

New Journal of Physics
The open access journal at the forefront of physics

Deutsche Physikalische Gesellschaft DPG
IOP Institute of Physics

Published in partnership with: Deutsche Physikalische Gesellschaft and the Institute of Physics

OPEN ACCESS

RECEIVED
7 June 2016

REVISED
8 August 2016

ACCEPTED FOR PUBLICATION
12 August 2016

PUBLISHED
6 September 2016

PAPER

Surface state conductivity in epitaxially grown $Bi_{1-x}Sb_x(111)$ films

Julian Koch[1], **Philipp Kröger**[1], **Herbert Pfnür**[1,2] **and Christoph Tegenkamp**[1,2]

[1] Institut für Festkörperphysik, Leibniz Universität Hannover, Appelstraße 2, D-30167 Hannover, Germany
[2] Laboratory of Nano and Quantum Engineering (LNQE), Leibniz Universität Hannover, Schneiderberg 39, D-30167 Hannover, Germany

E-mail: tegenkamp@fkp.uni-hannover.de

Keywords: thin films, topological insulator, surface transport

Abstract

Topologically non-trivial surface states were reported first on $Bi_{1-x}Sb_x$ bulk crystals. In this study we present transport measurements performed on thin $Bi_{1-x}Sb_x$-films (up to 24 nm thickness) grown epitaxially on Si(111) with various Sb-concentrations (up to $x = 0.22$). The analysis of the temperature dependency allowed us to distinguish between different transport channels originating from surface and bulk bands as well as impurity states. At temperatures below 30 K the transport is mediated by surface states while at higher temperatures activated transport via bulk channels sets in. The surface state conductivity and bulk band gaps can be tuned by the Sb-concentration and film thickness, respectively. For films as thin as 4 nm the surface state transport is strongly suppressed in contrast to Bi(111) films grown under identical conditions. The impurity channel is of intrinsic origin due to the growth and alloy formation process and turns out to be located at the buried interface.

1. Introduction

The peculiar spin texture of surface states in topological insulators (TI) sustainably triggers research activities [1]. The recent realizations of the quantum spin Hall effect [2] and the anomalous quantum Hall effect [3] by HgTe-films and ferromagnetic TIs, respectively, indicate the potential of this emergent material class. Recently, this topological classification scheme was successfully applied to Weyl semimetals [4].

However, a broadband use of this fascinating material, where the electronic bulk bands are intimately related to the surface band structure, is to date missing. Most of these materials suffer from defects resulting in non-insulating bulk phases and also from low mobility surface transport. To some extent the effects of considerably high vacancy and interstitial defect concentrations can be overcome using compensated materials, e.g. Bi_2Te_2Se [5, 6].

Against this background the use of epitaxial films is a promising alternative [3, 7, 8]. So far mainly binary chalcogenide alloys (Bi_2Se_3, etc.) were grown by epitaxy on various substrates, e.g CdTe, AlN, and sapphire [9–12]. The technique of thin film growth allows both to grow high quality films and to further tailor the band structure by quantum size effects [13]. For instance, epitaxial layers of Bi_2Te_3 grown on $BaF_2(111)$ substrates reveal mobilities up to 4600 $cm^2\ Vs^{-1}$ at 14 K [14]. Moreover, this technique is well suited to control the surface stoichiometry and morphology, thus avoiding problems of termination which may occur during the cleavage process of bulk materials as confirmed for $TlBiSe_2$ [15, 16].

Non-trivial surface states were first demonstrated for bulk $Bi_{1-x}Sb_x$. Angle resolved photoemission (ARPES) performed on bulk materials revealed 5 surface state Fermi crossings in between the $\overline{\Gamma}$- and $\overline{M}$-point of the (111) oriented surface [1, 17]. Latest high resolution ARPES measurements performed on epitaxial films showed that the non-trivial character is maintained only by two surface states [18], in consistency with theory. An alleged third surface state found on bulk samples [17] turns out to be induced by bulk defects, supporting the general trend that epitaxial films exhibit less imperfections. $Bi_{1-x}Sb_x$ is attractive not only because of the expected high mobilities in the range of $10^4\ cm^2\ Vs^{-1}$ [19], but also because of the tunability to convert a (trivial) semimetal into a non-trivial direct band semiconductor at moderate doping concentrations in the range of $x = 0.07$–0.22 [18, 20, 21]. $Bi_{1-x}Sb_x$ alloys were subject to transport experiments already 20 years ago, however, with the

emphasis of their thermoelectric properties. Interestingly, an impact of the robust topologically protected surface state in this material system was neither proven nor considered so far in transport experiments. Instead, the transport findings were discussed in terms of impurity and bulk bands [9, 21]. Moreover, quantum size effects in thin films should severely affect the band gaps as shown by a recent theoretical work [13].

In this study we focus on thin epitaxial $Bi_{1-x}Sb_x$ films grown on Si(111) substrates. The growth and morphology of the films was controlled by low energy electron diffraction. The systematic variation of film thickness, substrate temperature and Sb concentration allowed us to identify different transport channels. In particular, the low temperature conductance is governed by the surface states, which is effectively suppressed for 10 BL thin films. By quantum confinement the bulk contribution due to thermal excitation were shifted to higher temperatures, thus the rise in conductance seen at around 30 K is rather mediated by charge excitations from impurity bands. In contrast to former studies, we explain the metallic transport behavior seen below 30 K due to electron–phonon coupling of carriers in the surface state rather than due to the degenerate doping.

2. Experimental setup

All experiments were performed under ultra high vacuum conditions at a base pressure of 5×10^{-9} Pa. For the conductance measurements low-doped Si(111) samples (resistivity $\rho > 1000\ \Omega$ cm) were used. The samples are $15 \times 15 \times 0.5$ mm^3 in size and are provided with four slits and eight $TiSi_2$ contacts for transport measurements. Details about the fabrication of contacts as well as the *in situ* cleaning procedures are described elsewhere [22].

Bi and Sb were evaporated from Knudsen cells. The amounts were controlled by quartz microbalances while the stoichiometry and homogeneity of the binary compound were carefully checked (after *ex situ* transfer) by x-ray photoelectron spectroscopy (XPS) and sputter-XPS, respectively.

Both $Bi_{1-x}Sb_x$ and Bi(111) films (for reference), were grown at 200 k followed by annealing to 450 k for around 1 hour. The layer thickness of the Bi and $Bi_{1-x}Sb_x$ films are given in bilayers (BL $= 1.14 \times 10^{15}$ atoms cm^{-2}, deposition rate 1–2 BL per minute). The Bi and Sb coverage was calibrated with the help of the $\sqrt{3} \times \sqrt{3}$ reconstructions on Si(111) and by recording bilayer oscillations in conductance during evaporation at around 100 K.

The morphologies of the Si-substrates and the epitaxial films were checked by high-resolution low energy electron diffraction (SPA-LEED). The transport setup allows us to measure the conductance G as a function of coverage as well as temperature down to 10 K. In order to avoid repetitions we refer the interested reader to [22, 23].

3. Results and discussion

3.1. Surface structure

The co-deposition of Bi and Sb on Si(111) results in the growth of epitaxial films. In general, the quality of the surface structure depends sensitively on the film thickness and, to a lesser extent, on the stoichiometry.

For Sb-concentrations ranging between $x = 0.14$–0.19, at which this material class is in the inverted band gap phase regime [20, 21], films with (111)-orientation are grown as shown in figure 1. However, an increase of the film thickness is accompanied by an increase of the rotational disorder, at least if the annealing times for the films are kept constant. For instance, a 60 BL (24 nm) thick film shows almost arbitrarily oriented domains (see figure 1(d). In order to quantify the disorder we plotted in figure 1(g) azimuthal scans through the first order diffraction spots for various film thicknesses. Nonetheless, the sizes of the domains is in the order of 20 nm for all film thicknesses as deduced form the width at half maximum of the specular diffraction peak at an out-of phase scattering condition [24]. Thus, the rotational disorder is rather induced by the formation of an alloy than due to surface roughening upon growth.

In fact, that structural disorder is a result of the alloy formation, is in line with the growth mode found for Bi on Si(111): A 40 BL Bi-film, shown in figure 1(e), which has nominally a larger misfit to Si(111), reveals almost no rotational disorder [22, 25]. For reasons of comparison the Bi-film was grown at the same conditions, i.e. substrate temperature and growth rate.

Also the interface is crucial as was demonstrated by the so-called allotropic phase transition reported for epitaxial Bi(111) layers [26, 27]. It is likely that similar scenarios play a role for the growth of $Bi_{1-x}Sb_x$ films as well. For instance, the rotational disorder of a 50 BL thick $Bi_{1-x}Sb_x$-film is significantly reduced (see figure 1(f)), if growth is performed on a Bi(111) buffer layer (here 10 BL). Similarly grown films were used for the ARPES studies [18]. However, for our transport investigations buffer-layer free $Bi_{1-x}Sb_x$ films are mandatory.

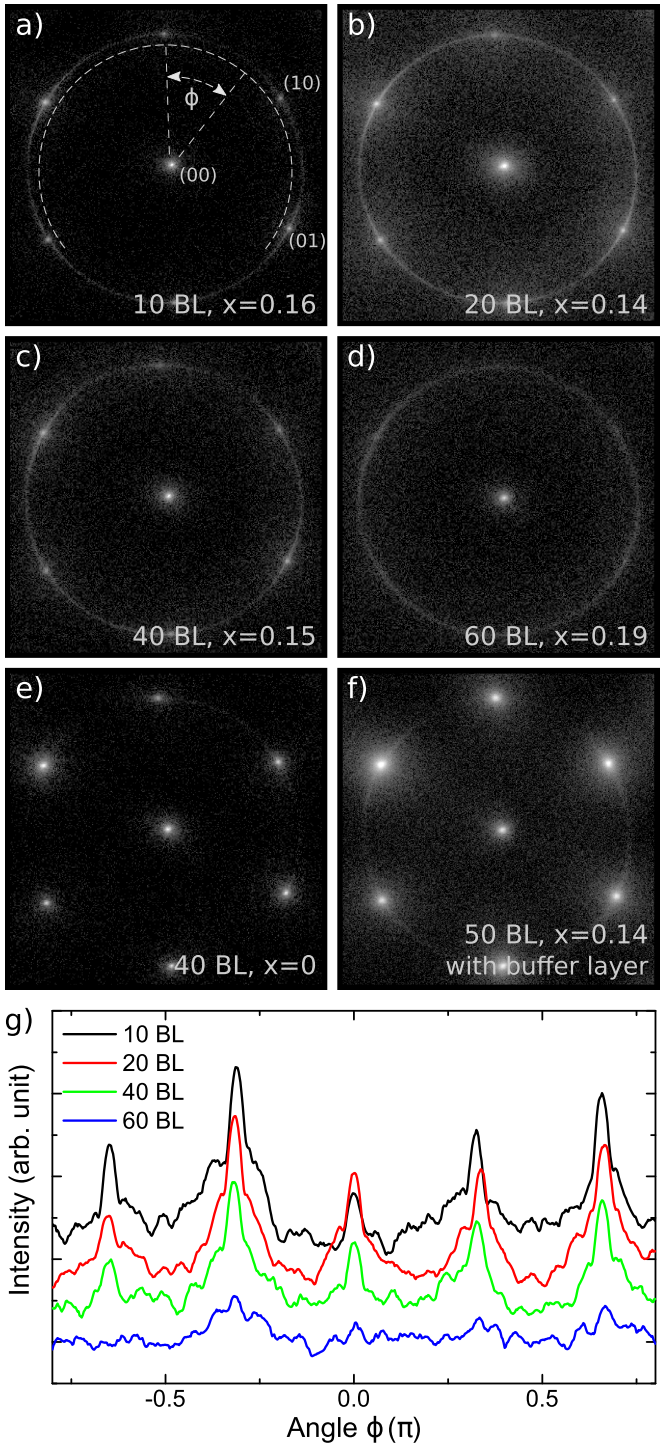

Figure 1. SPA-LEED diffraction patterns of $Bi_{1-x}Sb_x$ (111)-films (a)–(d), pure Bi(111) (e) and a $Bi_{1-x}Sb_x$-film with a 10 BL Bi-buffer layer (f) grown on Si(111). The electron energy was 87 eV (95 eV in (f). The thicknesses of the films as well as the Sb-concentrations x are indicated. (g) Azimuthal line scans (shifted for better visibility) taken along the first order diffraction spots shown in (a)–(d). The scan direction is roughly indicated in (a) by the dashed circle.

3.2. DC *in situ* transport in epitaxial $Bi_{1-x}Sb_x$ films

3.2.1. Size effects and temperature dependency

In the following, we show results of surface sensitive transport measurements, which were performed on epitaxial $Bi_{1-x}Sb_x$ films directly grown on Si(111). The conductance measured for the clean Si-substrate in the temperature interval up to 300 K was below 10 μS and is therefore negligible. Figure 2(a) shows the conductance G as a function of temperature T for variously thick films (20–60 BL). The electronic band structure for the non-trivial case is depicted in the inset of figure 2. Based on our sample geometry and film thicknesses the conductance values correspond to a resistivity in the order of $\mu\Omega$ m, which is in reasonable agreement with results obtained for bulk

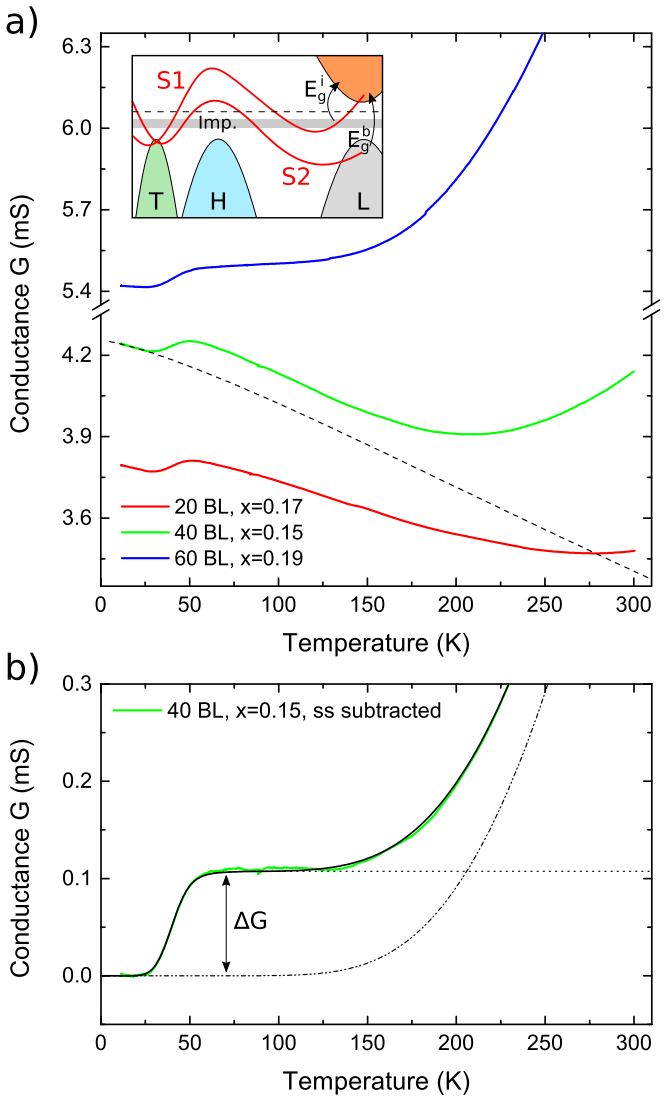

Figure 2. (a) Conductance G as a function of temperature for $Bi_{1-x}Sb_x$ films of various thicknesses. The dashed line shows the contribution of the surface state (ss). Inset: electronic band structure for the non-trivial scenario showing five Fermi level (dashed line) crossings with two surface states $S1$ and $S2$. The figure was reproduced from [18]. In addition we plotted the position of an impurity (imp.) band (not to scale). For further details see text. (b) G of a 40 BL film after subtraction of the ss-contribution. The dotted and dashed–dotted curves are fits taking into account thermal activation of carriers from impurity (E_g^i) and valence bulk bands (E_g^b), respectively.

materials [9, 21]. The Sb-concentration of the films shown in figure 2 is quite similar, and thus cannot account for the difference in the absolute values of the conductances. As we will show below, the influence on the conductance due to the variation of the Sb concentration in this regime ($x = 0.15$–0.19) is less than 5%.

Albeit the absolute conductance values are different, the $G(T)$-curves reveal similarities: at low temperatures the conductance decreases with increasing temperature and reaches a minimum at around 30 K, after which the conductance increases until $T \approx 50$ K. At high temperatures there is a second increase, that becomes more pronounced with increasing film thickness. For the 20 BL film only the tendency of this increase at around 270 K is visible. Referring to the temperature-dependent transport measurements done on Bi thin films, complemented by charge carriers generated from impurities (third term), the conductance can be accurately modeled in our case via [28, 29]:

$$G(T) = [G_0^{-1} + aT^m]^{-1} + b \cdot \exp\left(-\frac{E_g^b}{2k_B T}\right) + 2\Delta G\left[1 + \left[1 + 4cT^{-3/2}\exp\left(\frac{E_g^i}{2k_B T}\right)\right]^{1/2}\right]^{-1}$$

k_B denotes the Boltzmann factor and a, b, c are constants. Details are explained in the following: the first term describes the metallic surface transport (G_0 refers to the surface conductance at 0 K) including electron–phonon scattering within the surface transport channel. The dashed line with the exponent $m = 1.3$ in figure 2(a) shows the fit of this contribution to the $G(T)$-curve of the 40 BL film .

The second and the third term describe activated transport channels characterized by their gap energies E_g^b and E_g^i and correspond to the high and low temperature rises in conductance, respectively. For the sake of simplicity a coupling to the phonon bath was neglected for both terms The bulk Debye temperature is around 200 K, i.e. phononic contributions of the charge carrier mobility are not dominating the transport in the low temperature range. This is reflected also by the exponent m, which only slightly deviates from $m = 1$ found for the surface contribution in Bi nanostructures [28]. Moreover, contributions due to hopping via defects within the films are not considered at the moment. Despite these simplifications, the $G(T)$-curves are excellently described over the entire temperature range as shown for the 40 BL film in figure 2(b), where ΔG represents the increase of the conductance.

In former studies only one activated transport channel at around 30 K was observed which is attributed to thermal activation of charge carriers from bulk valence bands into the conduction band channels [9, 21, 37–40]. In this study, only the rise in conductance at high temperatures corresponds to activated bulk transport while the rise at low temperature is of different origin. This interpretation is motivated by the fact that the minimum at 30 K is independent of the film thickness. If bulk states are involved, the minimum should shift to lower temperatures with increasing film thickness [28]. The gap energies deduced from the low temperature regime were found to be $E_g^i = 38 \pm 3$ meV and are too small according to calculations of the renormalization of the bulk bands due to quantum confinement [13]. Moreover, the increase of the conductance $\Delta G = 100 \pm 10$ μS for the low temperature activation channel was found to be rather similar in all films investigated here. There is also no correlation of ΔG with the rotational disorder of the films. Therefore, the low temperature rise is most likely not related with the surface structure and rather a bulk related feature, although unexpectedly independent on the film thickness. We will discuss this in more detail below in context of figure 4.

A size effect is seen in our experiments only for the activated channel at higher temperatures. The gap energies E_g^b deduced from transport for the 20, 40 and 60 BL thick films are 280 ± 70, 200 ± 20 and 160 ± 10 meV, respectively. Hence, the gap energy E_g^b scales inversely with the film thickness d. It follows that $E_g^b - E_0 \propto d^{-0.61}$ where $E_0 = 30$ meV denotes the bulk band gap, deduced in former studies [21]. The magnitude of the scaling power is lower compared to values measured for Sb doped SnO_2 ($\propto d^{-1.56}$) or InSb ($\propto d^{-1.4}$) thin films [30, 31]. However, the renormalization of the bulk band gap due to quantum confinement is at least for the 60 BL thick film in reasonable agreement with the calculations done for a trigonally oriented, free-standing film, neglecting any interface effects [13]. Moreover, as claimed by Tang *et al* [13] the bulk band structure depends on temperature above 77 K. This effect is not taken into account by our analysis and might be also responsible for the difference of exponent compared to other studies.

3.2.2. Surface state transport

In order to show that the low temperature conductance below 30 K is dominated by metallic surface transport, we first look at the conductance measured at 12 K, where the contributions of the activated transport channels to the overall conductance are negligible. As shown in figure 3(a) for 20, 40 and 60 BL thick films, G (12 K) increases sublinearly with increasing films thickness (the 10 BL film is a special case and will be discussed below). A similar behavior was found for epitaxial Pb- and Bi-films grown on Si substrates [32, 33]. A deviation from a strict linear behavior of the conductance with thickness is expected if surface and interface scattering is important [34, 35]. The fact that the conductance depends also on the film thickness clearly shows that transport through the bulk is present, even at these low temperatures. However, the increase in conductance is much smaller than expected if only bulk channels are present, thus both surface and bulk channels are contributing. Most likely the bulk contributions are caused by hopping transport across imperfections, e.g. stoichiometric disorder within the alloy or even crystallographic defects due to the lattice mismatch with the Si(111) substrate. As already mentioned, the variation of the Sb-concentration ($x = 0.15$–0.19) for the curves shown in figure 3(a) is too small in order to explain the thickness dependency.

To quantify these bulk-related defect channels further we performed conductance measurements at 12 K while growing a $Bi_{0.84}Sb_{0.16}$ film (figure 3(b)). To ensure a quasi layer-by-layer growth, the experiment was done on a 10 BL thick $Bi_{0.84}Sb_{0.16}$ buffer film which was prepared and annealed before the subsequent growth at low temperatures. The quality of the surface morphology at these conditions is rather poor and no sharp reflexes were visible in LEED. The measured curve shows a quasi linear increase of around 0.44 mS/10 BL. The overall lower conductance in comparison to figure 3(a) is in agreement with the non-crystalline structure and shows that extended surface states are not highly developed under these growth conditions. According to the extrapolation sketched by the dashed line in figure 3(b), thin $Bi_{1-x}Sb_x$ films should exhibit roughly twice as much parasitic bulk transport channels (1 mS/10 BL). This finding is qualitatively in agreement with our LEED

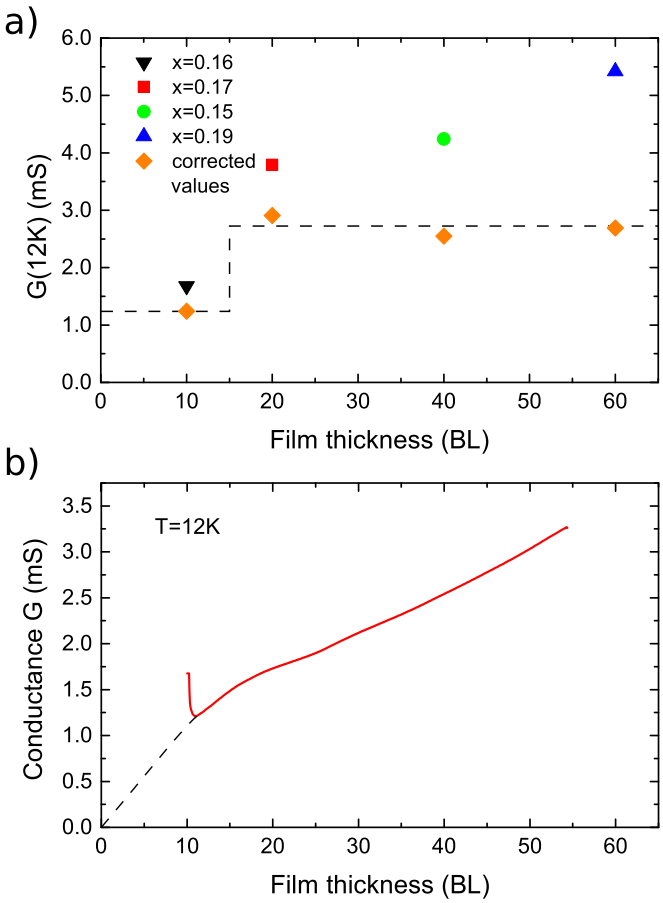

Figure 3. (a) Conductance G measured at 12 K as a function of film thickness. The corrected values denote the transport through the surface channel after subtracting parasitic bulk contributions. For further details see text. (b) Conductance measured during growth of a $Bi_{0.84}Sb_{0.16}$ film at 12 K. In order to reveal a quasi layer-by-layer growth at these low temperatures the evaporation was done on a pre-annealed 10 BL $Bi_{0.84}Sb_{0.16}$ buffer layer. The penetration of the surface state due to adsorption is seen by the initial drop in conductance. The dashed line is a guide to eye showing that the parasitic bulk contribution within the first 10 BL is almost larger by a factor of 2.

results revealing no crystalline surface structures for films below 10 BL and also with a significantly larger ΔG for a 10 BL thick film (see discussion in context of figure 4).

Based on these parasitic transport channels, the values discussed in the context of figure 3(a) can be corrected with respect to the bulk contribution. As obvious, the corrected values are independent of the film thickness for films thicker than 20 BL. This is expected if transport via surface states is dominant. The value of 2.8 mS refers to a surface conductivity of around 0.7 mS/□ and is approximately twice as high as the conductivity we measured for Bi(111) surface states [22].

Contrary to our interpretation, the qualitatively similar behavior found for bulk materials was assigned to an impurity band that overlaps with the fundamental conduction bulk band [21]. Generally, the high dielectric constant and low effective masses in $Bi_{1-x}Sb_x$ can provide extremely low ionization energies (≈10 μeV) and large Bohr radii (≈500 nm), thus even in almost pure material systems the heavy doping condition can be easily satisfied giving rise to such a parasitic transport channel [21]. A similar behavior of the conductivity was also reported when alloying Bi with a variety of elements, e.g. Pb, Sn, Zn or In [41]. Moreover, the importance of this impurity band was also reported for $Bi_{1-x}Sb_x$ thin films as well as nanostructured samples [9, 37]. Surprisingly, transport via robust surface states, as they were seen in spectroscopy [17], was not taken into account in these former transport studies.

We mentioned above that the conductance for a 10 BL thick TI-film at 12 K is, compared to thicker films, disproportionally reduced and we ascribe this to hybridization of the surface states. A similar behavior was found by Taskin *et al* in transport measurements in epitaxially grown Bi_2Se_3 films, where the metallic surface transport is diminished below a film thickness of 6 nm [12]. In our case, the suppression of the metallic surface transport occurs at roughly the same thickness (10 BL ≙ 4 nm). Evidence for this pronounced hybridization between the surface and interface states is found when looking at the temperature dependence of its conductance as shown in figure 4(a). The metallic signature of the surface transport channel, i.e. the decrease of the conductance at low

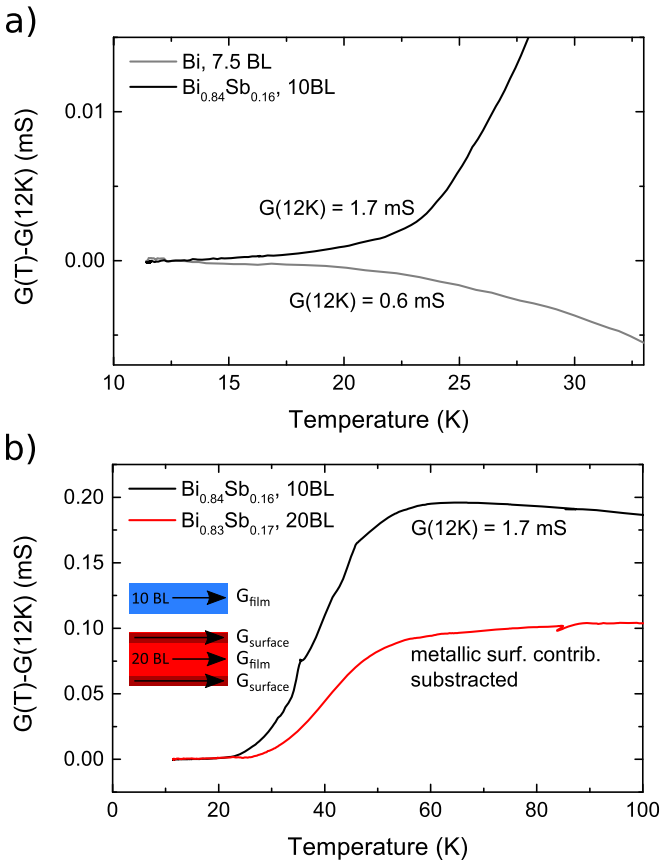

Figure 4. (a) Transport in thin $Bi_{1-x}Sb_x$ films. The metallic signature at low temperatures for the surface states is not seen for a 10 BL thick film while it is present for even thinner Bi-films. (b) For the 10 BL $Bi_{1-x}Sb_x$ films the ΔG is significantly larger than for a 20 BL thick film. In order to compare both films, the entire $G_{surface}(T)$ background was subtracted for the 20 BL film. The extrapolation shown in figure 3 suggested already that the defect concentration in thin structures is disproportionally high.

temperatures, is entirely missing for the 10 BL film, albeit the quality of the surface morphology is similar to that of a 20 BL thick film (see LEED in figure 1). In contrast, topologically trivial Bi(111) films, which are even thinner, still reveal the metallic fingerprint as shown in figure 4(a) [22, 32]. This finding supports our conclusion from above that the low temperature behavior of the conductance of $Bi_{1-x}Sb_x$ films (>20 BL) is dominated by metallic surface transport.

We mentioned above, that the ΔG contribution due to the impurity channel is rather independent of the film thickness. An exception is a 10 BL thin film which shows a ΔG significantly larger contribution compared to a 20 BL thick film as shown in figure 4(b). We attribute this to an increased disorder in thin film structures. A similar behavior was seen also for Bi epitaxy on Si(111). In this case a so-called allotropic transformation was reported [27], where in the course of deposition the initial pseudocubic growth becomes instable and the entire volume of the film starts to transform in a (111)-oriented, but strongly lattice-mismatched film. It is likely, that similar allotropic transitions play a role for $Bi_{1-x}Sb_x$ films as well. In any case, such effects could explain a higher bulk defect concentrations close to the interface.

3.2.3. Tuning of the surface state conductivity by the Sb-concentration

We will now discuss in more detail the influence of the Sb-concentration on the transport properties. All experiments were performed on 20 BL films which revealed a well-defined single domain structure in LEED. Figure 5(a) shows $G(T)$-curves for various Sb-concentrations. For reference, also a $G(T)$-curve for a 20 BL thick Bi(111) film is shown. Apparently, the conductance increases with increasing Sb concentration. While the curves for Bi and $Bi_{1-x}Sb_x$ look similar in the low temperature regime (up to 50 K) they reveal differences for higher temperatures as the quantum size induced renormalization of the band gap is smaller for Bi compared to $Bi_{1-x}Sb_x$. The analogue analysis revealed for Bi a gap energy $E_{g,Bi} \approx 50$ meV which is in good agreement with measurements regarding the semimetal-semiconductor transition performed on Bi nanostructures [28].

We mentioned that the low temperature regime is dominated by surface transport. The values obtained for various Sb concentrations up to $x = 0.22$ are shown in figure 5(b). Despite an expected increased scattering rate

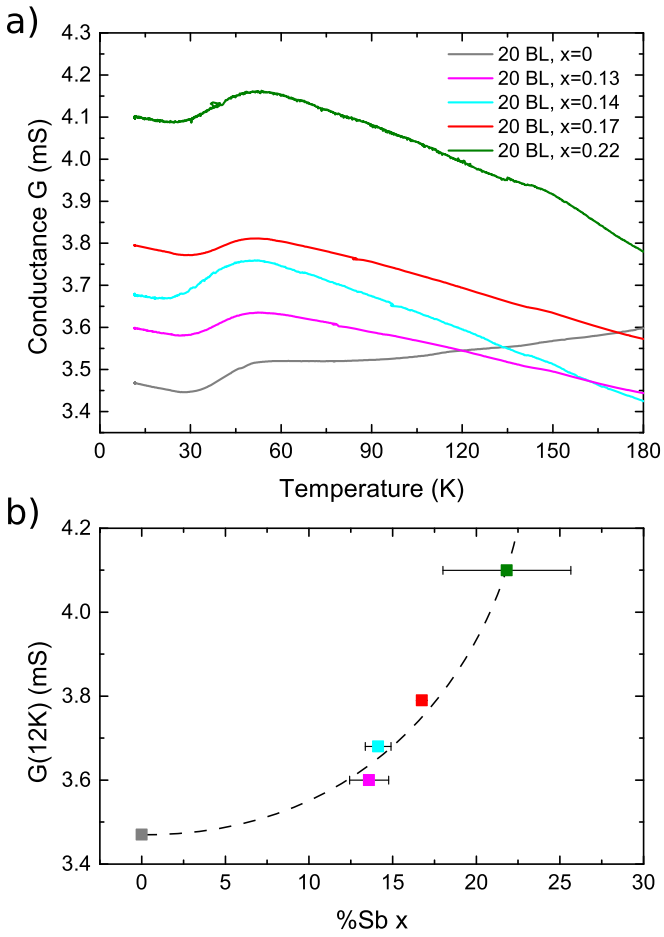

Figure 5. (a) Conductance as a function of temperature for 20 BL thick films and various Sb-concentrations. (b) Conductance at 12 K versus the Sb-concentration. The parasitic bulk contribution was not subtracted. The dashed line is a guide to the eye.

for the charge carriers in an alloyed phase the conductance increases, confirming a certain robustness of the surface states.

The gradual increase of the Sb concentration comes along with an increased band filling of the surface states. Benia *et al* [18] carefully investigated the band structure of similarly grown TI films. With increasing Sb concentration from $x = 0$ to $x = 0.25$ the Fermi wavevector k_F at $\bar{\Gamma}$ increases isotropically by around 23%. Consequently, the carrier concentration is increased by almost 50%. As can be seen from figure 5(b) the increase in the conductance in our case is less (only 20%) and most likely due to a superimposed decrease of the carrier density around the $\overline{M}$ point [18]. Moreover, first magneto transport revealed (not shown here) that also the carrier mobilities are reduced with increasing Sb concentration, which is in agreement with ARPES showing higher effective masses for the charge carriers at k_F [18].

The $G(T)$-curves, shown in figure 5(a), were analyzed also with respect to the activation energy E_g^i. The fitting around the low temperature minimum revealed around 37 ± 7 meV and showed no clear trend with respect to the Sb-concentration. This supports our conclusion that the rise in conductance at 30 k should not be attributed to bulk band gap E_g^b, which reveals a variable gap by varying the Sb concentrations ranging between 7%–22% seen for bulk materials in the same temperature regime [20, 21, 36].

3.2.4. The origin of the impurity states

We showed that the low temperature transport behavior is carried by surface states, in agreement with recent ARPES measurements [18]. Moreover, in consistency with calculations [13], we clearly observed a quantum confinement for the bulk states. Nonetheless, in our thin films a finite contribution at 30 K remains which is inconsistent with the former interpretation and needs clarification.

The steep increase seen at 30 K and the subsequent saturation are reminiscent of an activation of excess carriers from impurity states well decoupled from bulk bands. Compared to the measurements done on bulk material the increase is much smaller and around 0.1 mS which refers to a conductivity of $\Delta\sigma = 100$ S cm^{-1}. Assuming a saturation effect due to a limited carrier concentration and mobilities of around 100 cm^2 Vs^{-1}, the

carrier concentration is in the order of 10^{18} cm^{-3}. However, it can not be directly related to the formation of an alloy since this increase is also observed for pure Bi (see figure 5(a).

From ARPES studies it is clear that the surface states are metallic, i.e. any thermal energy will rather cause electron–phonon scattering which lowers the conductance. Hence, if thermally induced exchange between bulk and surface states are excluded, the activated channel at low temperature is purely bulk related. However, ΔG should then increase with increasing film thickness, which is not supported by our experiments (see figure 2).

This puzzling finding can be understood only if we assume that the bulk mediated impurity bands are *inhomogeneously* distributed in the direction of film growth. We mentioned above that ΔG is only weakly dependent on the surface morphology. Therefore, the main contribution must be due to impurity states located at the interface. This is fully in line with the $G(T)$-analysis shown in context of figure 3(b) suggesting a higher defect concentration within the first 10 BL. A similar scenario was found for the growth of Bi on Si(111) [27].

4. Summary and conclusion

In summary, the surface transport properties of epitaxial $Bi_{1-x}Sb_x$ films were examined in detail by systematic variation of the film thickness and the film stoichiometry. The temperature dependency of the transport findings suggests that both surface and bulk transport channels are present in these films.

By means of ultra-thin epitaxial films we were able to identify different transport channels. Besides the transport along surface states, activation from impurity and bulk bands takes place. In contrast to previous transport measurements on bulk material, we showed that the metallicity at low temperatures stems rather from surface states while the impurity bands are energetically split off from the fundamental bulk bands and located close to the $Si/Bi_{1-x}Sb_x$ interface. Compared to bulk materials, the bulk band gaps are increased by a factor of five due to quantum size effects, in accordance with theory [13]. With increasing Sb concentration the conductivity of the surface transport channel increases. This is in line with recent ARPES measurements showing increased filling factors of the surface bands [18]. In contrast to epitaxial Bi(111) films grown also on Si(111) the conductivity in the surface state is higher and apparently rather insensitive to defects. Moreover, a suppression of the surface state contribution was seen only for the $Bi_{1-x}Sb_x$ films.

Albeit theses signatures are expected for topologically non-trivial surface states envisaged magneto transport measurements will give further insight into this interesting research topic. In general, there are strong indications that the impurity band is rather an intrinsic feature due to the necessity of the formation of an alloy. This may explain why many other TI-alloys, e.g. Heusler compounds, suffer from a non-insulating behavior of the bulk.

Acknowledgments

Financial support by the Deutsche Forschungsgemeinschaft is gratefully acknowledged. We also acknowledge the help from the IHP (Frankfurt, Oder), especially Gunther Lippert and Ioan Costina, who performed sputter-XPS experiments on various samples. The publication of this article was funded by the Open Access Fund of the Leibniz Universität Hannover.

References

[1] Hasan M Z and Kane C L 2010 *Rev. Mod. Phys.* **82** 3045
[2] König M, Wiedmann S, Brüne C, Roth A, Buhmann H and Molenkamp L W 2007 *Science* **318** 766
[3] Chang C-Z, Zhao W, Kim D Y, Zhang H, Assaf B A, Heiman D, Zhang S-C, Liu C, Chan M H W and Moodera J S 2015 *Nat. Mat.* **14** 473
[4] Xu S-Y *et al* 2015 *Science* **349** 613
[5] Mi J-L *et al* 2013 *Adv. Mater.* **25** 889
[6] Barreto L *et al* 2014 *Nano Lett.* **14** 3755
[7] Partin D L, Thrush C M, Heremans J, Morelli D T and Olk C H 1988 *J. Vac. Sci. Technol.* B **7** 348
[8] Heremans J, Partin D L, Thrush C M, Karczewski G, Richardson M S and Furdyna J K 1993 *Phys. Rev.* B **48** 11329
[9] Cho S, DiVenere A, Wong G K and Ketterson J B 1999 *Phys. Rev.* B **59** 010691
[10] Tsipas P *et al* 2014 *ACS Nano* **8** 6614
[11] Lee Y F, Punugupati S, Wu F, Jin Z, Narayan J and Schwartz J 2014 *Curr. Opin. Solid State Mater. Sci.* **18** 279
[12] Taskin A A, Sasaki S, Segawa K and Ando Y 2012 *Phys. Rev. Lett.* **109** 066803
[13] Tang S and Dresselhaus M 2012 *Phys. Rev.* B **86** 075436
[14] Hoefer K *et al* 2014 *Proc. Natl Acad. Sci.* **111** 14979
[15] Kuroda K *et al* 2013 *Phys. Rev.* B **88** 245308
[16] Pielmeier F *et al* 2015 *New J. Phys.* **17** 023067
[17] Hsieh D *et al* 2008 *Nature* **452** 970
[18] Benia H M, Straßer C, Kern K and Ast C R 2015 *Phys. Rev.* B **91** 161406(R)
[19] Taskin A A *et al* 2010 *Phys. Rev.* B **82** 121302(R)
[20] Fu L and Kane C L 2007 *Phys. Rev.* B **76** 045302

[21] Lenoir B, Cassart M, Michenaud J-P, Scherrer H and Scherrer S 1996 *J. Phys. Chem. Solids* **57** 89
[22] Lükermann D, Sologub D, Pfnür A and Tegenkamp C 2011 *Phys. Rev.* B **83** 245425
[23] Lükermann D *et al* 2012 *Phys. Rev.* B **86** 195432
[24] Horn-von Hoegen M 1999 *Z. Kristallogr.* **214** 591
[25] Klein C *et al* 2015 *Phys. Rev.* B **91** 195441
[26] Nagao T *et al* 2005 *Surf. Sci.* **590** L247
[27] Nagao T *et al* 2004 *Phys. Rev. Lett.* **93** 105501
[28] Xiao S, Wei D and Jin X 2012 *Phys. Rev. Lett.* **109** 166805
[29] Gross R and Marx A 2012 *Solid State Physics* (Munich: Gruyter Oldenbourg)
[30] Ke C, Zhu W, Zhang Z, Tok E S and Ling B 2015 *J. Pan. Sci. Rep.* **5** 17424
[31] Berchtold K and Huber D 1969 *Phys. Stat. Sol.* **33** 425
[32] Hirahara T *et al* 2007 *App. Phys. Lett.* **91** 202106
[33] Lükermann D, Pfnür H and Tegenkamp C 2010 *Phys. Rev.* B **82** 045401
[34] Fishman G and Calecki D 1989 *Phys. Rev. Lett.* **62** 1302
[35] Calecki D 1990 *Phys. Rev.* B **42** 6906
[36] Gou H *et al* 2011 *Phys. Rev.* B **83** 201104(R)
[37] Will C H *et al* 2013 *J. Appl. Phys.* **114** 193707
[38] Jain A L 1959 *Phys. Rev.* **114** 1518
[39] Yim W M and Amith A 1972 *Solid-State Electron.* **15** 1141
[40] Morelli D T, Partin D L and Heremans J 1990 *Semicond. Sci. Technol.* **5** 257
[41] Thompson N and Wills H H 1935 *Proc. R. Soc.* A **155** 111